Article ID: 1000-7032(2024)12-1975-09

Hot Isostatic Pressing and Characterizations of Eu^{3+}-doped $(Gd,Lu)_2O_3$ Transparent Ceramics

LIU Qiang[1], HE Ningtong[1,2], WANG Yanbin[2,3], HUANG Dong[1,2], CHEN Yuyang[2,3], LI Tingsong[2], ZHOU Zhenzhen[2,3], HU Chen[2,3], IVANOV Maxim[4,5], LI Jiang[2,3*]

(1. *School of Material Science and Engineering, Jiangsu University, Zhenjiang* 212013, *China*;
2. *Transparent Ceramics Research Center, Shanghai Institute of Ceramics, Chinese Academy of Sciences, Shanghai* 201899, *China*;
3. *Center of Materials Science and Optoelectronics Engineering, University of Chinese Academy of Sciences, Beijing* 100049, *China*;
4. *Institute of Electrophysics, Ural branch of Russian Academy of Sciences, Ekaterinburg* 620016, *Russia*;
5. *Center of Excellence for Photoconversion, Vinča Institute of Nuclear Sciences — National Institute of the Republic of Serbia, University of Belgrade, Belgrade* 52211001, *Serbia*)

* *Corresponding Author, E-mail: lijiang@mail.sic.ac.cn*

Abstract: $(Gd,Lu)_2O_3$:Eu scintillation ceramics have promising applications in the high-energy X-ray imaging. $Eu_{0.1}Gd_{0.6}Lu_{1.3}O_3$ nano-powders with pure phase were prepared from the precursor calcined at 1 050 ℃ for 4 h by the co-precipitation method. Using the synthesized nano-powders as initial material, $Eu_{0.1}Gd_{0.6}Lu_{1.3}O_3$ ceramics were fabricated by vacuum pre-sintering at different temperatures for 2 h and hot isostatic pressing (HIP) at 1 750 ℃ for 3 h in argon. The influence of pre-sintering temperature on the microstructure, optical and luminescence properties was investigated. The $Eu_{0.1}Gd_{0.6}Lu_{1.3}O_3$ ceramics pre-sintered at 1 625 ℃ for 2 h combined with HIP post-treatment show the highest in-line transmittance of 75.2% at 611 nm. The photoluminescence (PL) and X-ray excited luminescence (XEL) spectra of the $Eu_{0.1}Gd_{0.6}Lu_{1.3}O_3$ transparent ceramics demonstrate a strong red emission peak at 611 nm due to the $^5D_0 \rightarrow {}^7F_2$ transition of Eu^{3+}. The PL, PLE and XEL intensities of the HIP post-treated $Eu_{0.1}Gd_{0.6}Lu_{1.3}O_3$ ceramics show a trend of first ascending and then descending with the increase of pre-sintering temperature. The thermally stimulated luminescence (TSL) curve of the HIP post-treated $Eu_{0.1}Gd_{0.6}Lu_{1.3}O_3$ ceramics presents one high peak at 178 K and two peaks with lower intensities at 253 K and 320 K. The peak at 320 K may be related to oxygen vacancies, and the luminescence peak at 178 K is related to defects caused by the valence state changes of Eu^{3+} ions.

Key words: $(Gd,Lu)_2O_3$:Eu; transparent ceramics; microstructure; optical properties; hot isostatic pressing
CLC number: O482.31 **Document code**: A **DOI**: 10.37188/CJL.20240186

Eu^{3+}掺杂$(Gd,Lu)_2O_3$透明陶瓷的热等静压烧结与性能表征

刘 强[1], 贺宁桐[1,2], 王雁斌[2,3], 黄 东[1,2], 陈宇洋[2,3], 李廷松[2], 周真真[2,3], 胡 辰[2,3], IVANOV Maxim[4,5], 李 江[2,3*]

(1. 江苏大学 材料科学与工程学院, 江苏 镇江 212013;
2. 中国科学院 上海硅酸盐研究所, 透明陶瓷研究中心, 上海 201899;
3. 中国科学院大学 材料科学与光电工程中心, 北京 100049;

收稿日期: 2024-08-03; **修订日期**: 2024-08-20
基金项目: 中国科学院国际合作项目(121631KYSB20200039); 上海市自然科学基金(22ZR1472100); 中国科学院国际人才计划(2024VEA0005,2024VEA0014)
Supported by the International Partnership Program of Chinese Academy of Sciences(121631KYSB20200039); the Natural Science Foundation of Shanghai(22ZR1472100); the Chinese Academy of Sciences President's International Fellowship Initiative(2024VEA0005,2024VEA0014)

4. 俄罗斯科学院 乌拉尔分院，电物理研究所，俄罗斯 叶卡捷琳堡 620016；
5. 贝尔格莱德大学塞尔维亚共和国国家研究所 Vinča 核科学研究所光转换卓越中心，塞尔维亚 贝尔格莱德 52211001）

摘要：$(Gd,Lu)_2O_3$:Eu 闪烁陶瓷在高能 X 射线成像技术应用中具有广阔的应用前景。采用共沉淀法合成的前驱体经过 1 050 ℃煅烧 4 h 后，制备出纯相的 $Eu_{0.1}Gd_{0.6}Lu_{1.3}O_3$ 纳米粉体。以合成的纳米粉体为原料，采用不同温度下真空预烧（保温 2 h）结合热等静压烧结（1 750 ℃×3 h，Ar 气氛）制备了 $Eu_{0.1}Gd_{0.6}Lu_{1.3}O_3$ 陶瓷。研究了预烧结温度对 $Eu_{0.1}Gd_{0.6}Lu_{1.3}O_3$ 陶瓷微观结构、光学和发光特性的影响。在 1 625 ℃下预烧 2 h 并结合 HIP 后处理的 $Eu_{0.1}Gd_{0.6}Lu_{1.3}O_3$ 陶瓷具有最高的直线透过率（75.2% @ 611 nm）。由于 Eu^{3+} 的 $^5D_0\rightarrow{}^7F_2$ 能级跃迁，HIP 后处理的 $Eu_{0.1}Gd_{0.6}Lu_{1.3}O_3$ 陶瓷的 PL 和 XEL 光谱均在 611 nm 处具有最强的红色发射峰，其强度随预烧温度的提高呈现出先上升后下降的趋势。$Eu_{0.1}Gd_{0.6}Lu_{1.3}O_3$ 陶瓷的热释光（TSL）曲线在 178 K 处呈现一个强度较高的峰值，在 253 K 和 320 K 处呈现两个强度较低的峰值。320 K 的峰值可能与氧空位有关。178 K 处的发光与 Eu^{3+} 离子本身价态变化引起的缺陷有关。

关 键 词：$(Gd,Lu)_2O_3$:Eu；透明陶瓷；微观结构；光学特性；热等静压烧结

1 Introduction

Inorganic scintillators are widely used in medical diagnostics, industrial non-destructive detection, nuclear physics and high energy physics[1-5]. Among sesquioxide, lutetium oxide is of significant interest due to its high density (ρ = 9.42 g/cm^3), high effective atomic number (Z_{eff} = 63), high X-ray attenuation cross section and high efficiency in converting X-ray radiation into visible light in the case of doping the material with rare earth ions. For example, Lu_2O_3:Eu^{3+} exhibits intense radio-luminescence at the wavelength of 611 nm, which matches well with spectral sensitivity range of modern Si-photodiodes and charge-coupled devices[6-7].

Despite many researches on the growth of Lu_2O_3 single crystals (SCs), it is difficult for Lu_2O_3 to be produced to SCs due to the high melting temperature (about 2 450 ℃)[8]. Thus, the preparation of Lu_2O_3 transparent ceramics can be an effective way to obtain optical bulk Lu_2O_3 material, which is attributed to the low temperature and short time of the preparation. Kopylov *et al.* [9] demonstrated a possibility of high-temperature (1 850 ℃) vacuum sintering of Lu_2O_3:Eu^{3+} (5%)(at.) ceramics from nano-powders obtained by co-precipitation method. The in-line transmittance of the ceramics achieved 41% in visible wavelength range. Qin *et al.* [10] proposed that solid solutions of $Gd_{2(1-x-y)}Lu_{2x}Eu_{2y}O_3$ can be used as scintillation materials. The $(Gd,Lu)_2O_3$:Eu ceramics were made by solid-state reaction at 1 600 ℃ for 10 h in air, and the $Gd_{1.1}Lu_{0.8}Eu_{0.1}O_3$ samples became translucent. Seeley *et al.* [11] investigated phase stabilization in $(Gd,Lu)_2O_3$:Eu ceramics in detail. Eu^{3+} ions tend to exsolve from the Lu_2O_3 cubic crystal lattice and concentrate at the grain boundaries, where it precipitated into a secondary monoclinic phase resulting in optical scattering. The addition of Gd^{3+} ions to the cubic lattice of Lu_2O_3 stretches the lattice by observing the grain boundaries through tests such as TEM, which allowed the larger Eu^{3+} ions to stay in the lattice and reduced the secondary phases. Also, the transparency of the ceramics has been improved. Nanoparticles with different $Gd_xLu_{1.9-x}Eu_{0.1}O_3$ composition were synthesized *via* the flame spray pyrolysis and the green body was vacuum pre-sintered at 1 625 ℃ for 2 h and then hot isostatic pressing (HIP) under 200 MPa of inert argon at temperatures ranging between 1 750 ℃ and 1 900 ℃ for 4 h. Then several $(Gd,Lu)_2O_3$:Eu scintillators with the diameter of 10 inch and the thickness of 0.1 inch were fabricated[12-13]. The high energy radiography of $(Gd,Lu)_2O_3$:Eu ceramics performs better than scintillation glass, due to higher light yield (55 000 ph/MeV) and better X-ray stopping power. Nevertheless, the HIP-ed $(Gd,Lu)_2O_3$:Eu ceramics have large average crystallite size (from hundreds of microns up to a millimeter range) and high porosity at edges of the crystallites, which seriously decreases mechanical, thermo-

mechanical and optical properties of the ceramics. Rétot *et al.* [14] prepared $(Lu_{0.5}Gd_{0.5})_2O_3$ ceramics. The addition of Gd^{3+} ions not only facilitated sintering of the ceramics but also reduced the persistent luminescence of Eu^{3+} ions. The transmittance of $(Lu_{0.5}Gd_{0.5})_2O_3:Eu^{3+}$ ceramics after HIP treatment reach 38% at the wavelength of 612 nm. Under X-ray excitation, the afterglow decreases by one order of magnitude within the time range of 3 ms to 300 ms. From all these studies, it becomes evident that the $(Gd,Lu)_2O_3$:Eu solid solution can be a good scintillation material, but it is necessary to significantly improve the technology for the fabrication of transparent ceramics to achieve high optical quality.

In our previous researches, the $(Gd,Lu)_2O_3$:Eu ceramics were fabricated by the solid-state reaction with long-time vacuum sintering[15-16]. However, the sintering ability was low, resulting in the presence of numerous internal defects in the samples after sintering. Thus, the in-line transmittance of ceramics was only 32.6%@611 nm. The key step in preparing ceramics with high optical quality is to prepare powders with high purity, small grain size and good dispersion[17-19]. Ping *et al.* [20] prepared well dispersed powders of $(Gd,Lu)_2O_3$:Eu with particle sizes ranging from 20–70 nm by co-precipitation method. Our research group had optimized the co-precipitation technique to fabricate oxide nano-powders of different compositions with small size, good dispersion and homogeneous elemental distribution[21-23]. The improved two-step sintering method has been applied in the preparation of transparent ceramics by vacuum pre-sintering and HIP post-treatment in an argon atmosphere[24-25].

In this study, the $Eu_{0.1}Gd_{0.6}Lu_{1.3}O_3$ nano-powders were fabricated by the co-precipitation method and the two-step sintering method was used to prepare the ceramics. The aim of this research is to investigate the influence of pre-sintering temperature on the microstructure, optical properties and scintillation characteristics of the $Eu_{0.1}Gd_{0.6}Lu_{1.3}O_3$ ceramics.

2 Experiment

The $(Gd,Lu)_2O_3$:Eu powders were prepared by the co-precipitation method. An appropriate amount of Eu_2O_3 (99.995%, shanghai Sheeny Metal Material co Ltd), Lu_2O_3 (99.995%, Shanghai Jingyun Material Technology Co., Ltd.) and Gd_2O_3 (99.999%, Jining Zhongkai New Materials Co., Ltd.) were dissolved in diluted nitric acid to obtain $Eu(NO_3)_3$, $Lu(NO_3)_3$ and $Gd(NO_3)_3$. The 500 mL of metal mixture solution was prepared at a concentration of 0.25 mol/L according to the $Eu_{0.1}Gd_{0.6}Lu_{1.3}O_3$ component. The 125 mL of $(NH_4)_2SO_4$ solution at a concentration of 1 mol/L was added to the metal mixture solution as a dispersant for the metal ions. The 600 mL of NH_4HCO_3 solution at a concentration of 1 mol/L was dropped into the mixed metal solution at a rate of 3 mL/min, which was used as a precipitant. After the titration process, the precursor solution was agitated for 10 min and then aged for 3 h. The precipitate was washed twice with an alcohol-water mixture (alcohol:water = 1:4). Then the precipitate was washed twice with alcohol and centrifuged. Finally, the precursor was dried in an oven at 70 ℃ for 18 h. The precursor was sieved through a 200-mesh sieve. The sieved precursor was calcined at 1 050 ℃ for 4 h in air to obtain pure phase $(Gd,Lu)_2O_3$:Eu powders. The powders were uniaxially pressed at 40 MPa into pellet shaped green bodies and then cold isostatically pressed (CIP) at 250 MPa. The green bodies were sintered at temperature of 1 600–1 675 ℃ for 2 h in a tungsten mesh-heated vacuum furnace (1×10^{-3} Pa). Then the ceramics were hot isostatically pressured (HIP) at 1 750 ℃ (176 MPa, Ar) for 3 h and annealed in air at 1 300 ℃ for 10 h. The ceramic samples were mirror-polished to 1.2 mm thickness for subsequent testing. The phase identification was performed by the X-ray diffractometry (XRD, D/max2200 PC, Rigaku, Japan) using Cu Kα radiation (λ = 0.154 06 nm) with a scanning speed of 5(°)/min in the 2θ range of 10°–80°. Micrographs of the precursors, powders and pre-sintered ceramics were observed by a field emission scanning electron microscopy (FESEM, SU9000, Hitachi, Japan). The micrographs of the HIP post-treated ceramics were observed with optical microscope (Olympus BX51 three-dimensional digital

stereomicroscope, American). To measure grain size, the ceramics after polishing were thermally etched at 1 450 ℃ for 3 h. The average grain size in the ceramics was measured by the linear intercept method, and calculated by multiplying the average linear intercept distance by 1.56. The density of the samples was calculated according to Archimedes' principle by the formula:

$$\rho = m_0\rho_0/(m_2 - m_1), \quad (1)$$

where m_0 is the mass of the dry sample in air, m_1 is the mass of the sample completely submerged in water after sufficient water absorption, m_2 is the mass of the sample absorbed sufficient water, and ρ_0 is the density of distilled water (1.0 g/cm^3). Relative density of the samples is $\rho_1=(\rho/\rho_{th})\times100\%$, and ρ_{th} is the theoretical density of the samples. The in-line transmittance of the samples was measured by a UV-visible-near-infrared spectrophotometer (Cary-5000 (Varian), USA). The photoluminescence excitation (PLE) and emission (PL) spectra were recorded using a Shimadzu RF-5301PC Spectro fluorophotometer. The X-ray excited luminescence (XEL) spectra were analyzed with an equipment composed of the medical F30III-2 mobile diagnostic X-ray machine (70 kV, 1.5 mA) and QE65000 spectrometer (Ocean Optics, U. S.). In addition, on top of the test system, the Oxford DN-V2 cryostat is equipped to perform thermally stimulated luminescence measurements on ceramic samples to analyze the types of defects present in the ceramics. The radioluminescence at different temperatures was monitored by the same device.

3 Results and Discussion

Fig. 1 shows the micrographs of $Eu_{0.1}Gd_{0.6}Lu_{1.3}O_3$ precursor and the powders calcined at 1 050 ℃ for 4 h. The synthesized powders consist of nanoscale particles. After calcination, most of the nanoparticles are polyhedral due to the formation of the crystal structure.

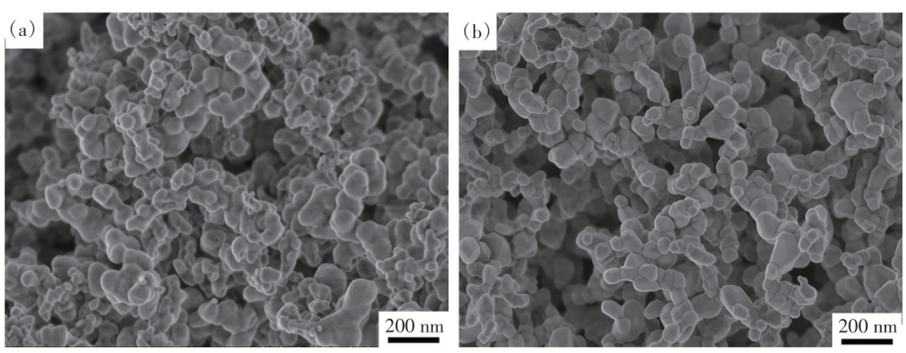

Fig. 1 FESEM micrographs of $Eu_{0.1}Gd_{0.6}Lu_{1.3}O_3$ precursor(a) and the powders(b) calcined at 1 050 ℃ for 4 h

Fig. 2 shows the XRD patterns of $Eu_{0.1}Gd_{0.6}Lu_{1.3}O_3$ precursor and the powders calcined at 1 050 ℃ for 4 h. The precursor was amorphous. The calcined powders have a cubic crystal structure with a space group of $Ia3$. The lattice parameter is 1.052 nm, which is larger than that of pure Lu_2O_3 (a = 1.026 nm). The ionic radius of Gd^{3+} (0.093 8 nm) is larger than that of Lu^{3+} (0.084 8 nm). The lattice parameter becomes larger with the addition of Gd^{3+} into the solid solution. The average crystallite size (D_{XRD}) of $Eu_{0.1}Gd_{0.6}Lu_{1.3}O_3$ calcined powders can be calculated from Fig. 1 by the Scherrer's equation:

$$D_{XRD} = 0.89\lambda/(\beta\cos\theta), \quad (2)$$

where λ is the wavelength of Cu Kα radiation, β is the full width at half maximum (FWHM) of a diffraction peak at Bragg angel (θ). The calculated

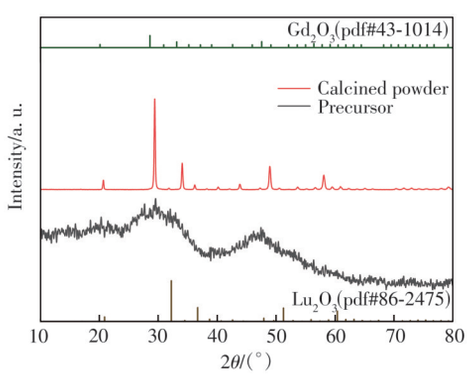

Fig. 2 XRD patterns of $Eu_{0.1}Gd_{0.6}Lu_{1.3}O_3$ precursor and the powders calcined at 1 050 ℃ for 4 h

average crystallite sizes of the $Eu_{0.1}Gd_{0.6}Lu_{1.3}O_3$ calcined powders are 41.9 nm.

Fig. 3 shows the relative densities of the $Eu_{0.1}Gd_{0.6}Lu_{1.3}O_3$ ceramics vacuum sintered at different temperatures for 2 h and the $Eu_{0.1}Gd_{0.6}Lu_{1.3}O_3$ ceramics HIP post-treated at 1 750 ℃ for 3 h. The relative densities of the $Eu_{0.1}Gd_{0.6}Lu_{1.3}O_3$ ceramics vacuum sintered above 1 600 ℃ for 2h are all above 94%, and the relative densities continue to increase with the increase of the sintering temperature. All $Eu_{0.1}Gd_{0.6}Lu_{1.3}O_3$ ceramic samples demonstrate the relative density reaches over 99% of the theoretical value after the HIP post-treatment.

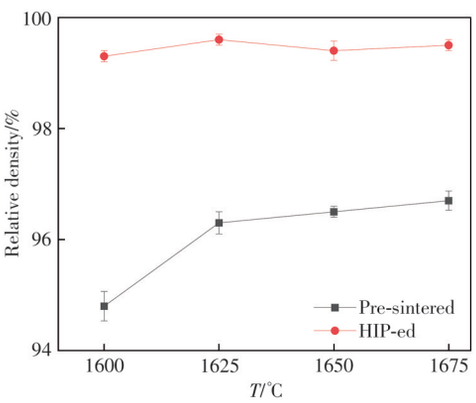

Fig. 3　Dependence of relative densities for the pre-sintered/HIP post-treated $Eu_{0.1}Gd_{0.6}Lu_{1.3}O_3$ ceramics on pre-sintering temperature

The morphologies of the $Eu_{0.1}Gd_{0.6}Lu_{1.3}O_3$ ceramics pre-sintered at different temperatures for 2 h are shown in Fig. 4. The sintering under vacuum conditions effectively removes gases, such as water vapor, hydrogen, and oxygen, which are present in the oxide ceramic billet. The grain boundary diffusion or gas escape from the ceramic billet leads to an increase in the product's density. The ceramics exhibit the uniform grain size. However, as the pre-sintering temperature increases, the grain size of the pre-sintered ceramic also enlarges. Concurrently, pores gradually accumulate within the ceramic matrix. As the sintering temperature rises, the average grain size of the ceramics increases from 740 nm to 2.3 μm.

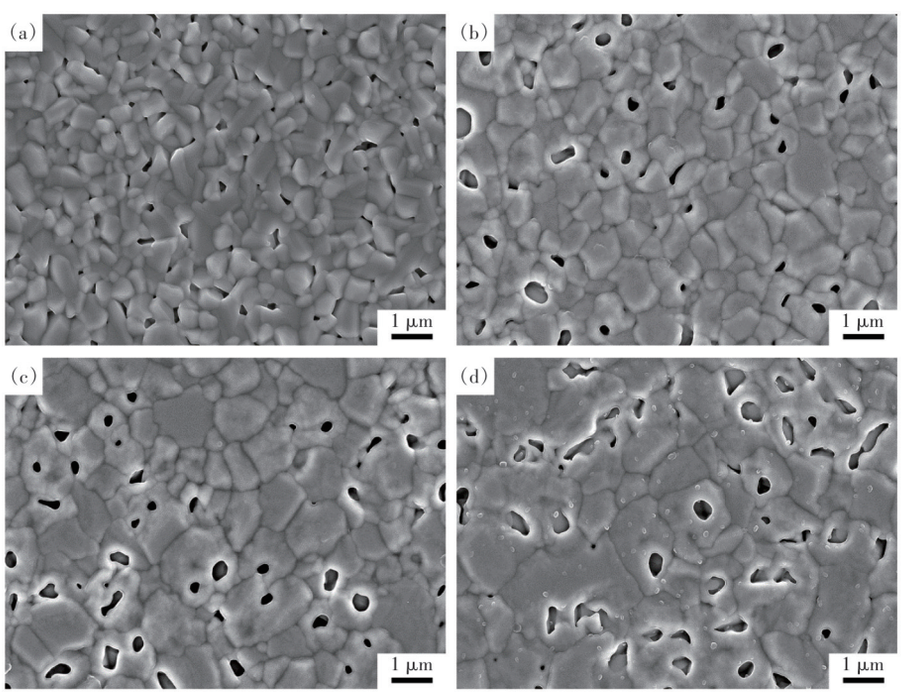

Fig. 4　FESEM micrographs of $Eu_{0.1}Gd_{0.6}Lu_{1.3}O_3$ ceramics pre-sintered at different temperatures for 2 h: (a)1 600 ℃, (b)1 625 ℃, (c)1 650 ℃, (d)1 675 ℃

Fig. 5 shows the optical microscopic images of the $Eu_{0.1}Gd_{0.6}Lu_{1.3}O_3$ ceramics pre-sintered at different temperatures for 2 h and HIP post-treated at 1 750 ℃ for 3 h under 176 MPa. The ceramics have uniform grain sizes. The average grain size of ceramics ranges from 56.6 μm to 81.3 μm with the increase of sintering temperature. At the pre-sintering temperature of 1 600 ℃, numerous pores are found

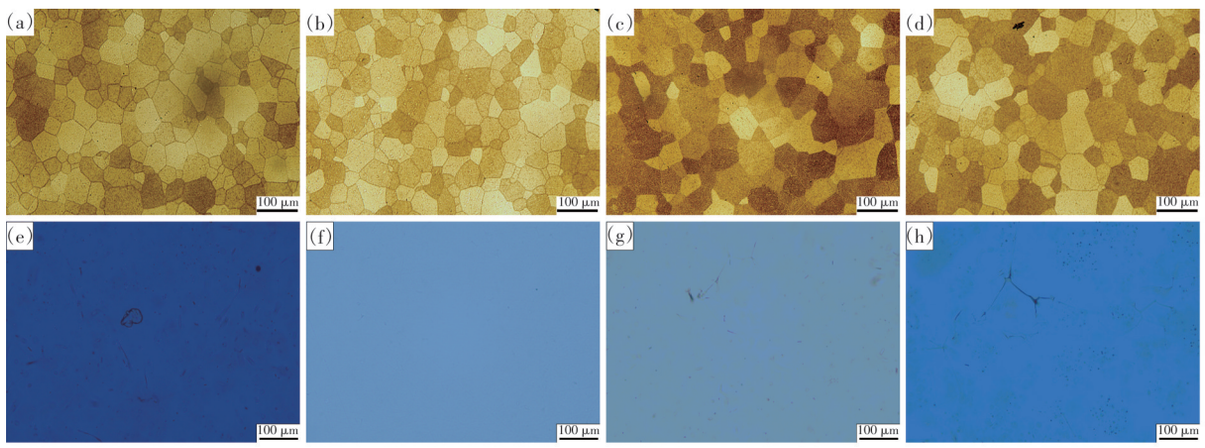

Fig. 5 Optical microscopic images of the $Eu_{0.1}Gd_{0.6}Lu_{1.3}O_3$ pre-sintered at different temperatures for 2 h and HIPed at 1 750 ℃ for 3 h under 176 MPa: (a), (e)1 600 ℃; (b), (f)1 625 ℃; (c), (g)1 650 ℃; (d), (h)1 675 ℃

within the ceramics. The elevated sintering temperature leads to an increase in the number of pores.

Fig. 6 shows the photograph and the in-line transmittance of the $Eu_{0.1}Gd_{0.6}Lu_{1.3}O_3$ ceramics (thickness of 1.2 mm) prepared by two-step sintering. As can be seen from Fig. 6, the in-line transmittance of the transparent ceramics first increases and then decreases with the increase of pre-sintering temperature. The $Eu_{0.1}Gd_{0.6}Lu_{1.3}O_3$ ceramics pre-sintered at 1 625 ℃ for 2 h combined with HIP post-treatment show the highest in-line transmittance of 75.2% at 611 nm, which is still lagged behind current commercial products from Lawrence Livermore National Laboratory, USA (81.2% at 611 nm 1.0 mm). At lower vacuum sintering temperatures, the relative densities of the pre-sintered ceramics are correspondingly low. Many pores exist in the ceramics. In the HIP process, the grain boundary migration is too fast and the pores inside the ceramics can not be completely removed in time, which resulted in the low transmittance of the ceramics. Although obvious pores are observed under the optical microscope, the ceramic grains are too large to be clearly observed under the scale of the optical microscope. However, as the subsequent annealing temperature increases, the expansion of the pores within the ceramics significantly affects the transmittance of the ceramics. As the sintering temperature increases, the pores inside the ceramic are continuously discharged. However, during the discharging process, some of the pores are wrapped by the grains. As can be seen in Fig. 4, the pores inside the pre-sintered ceramic keep getting bigger with the increase of the pre-sintered temperature. When the vacuum sintering temperature increases to 1 650–1 675 ℃, more pores are entrapped in the grains (Fig. 4(c), (d)). Some of these pores may remain in the ceramics after the HIP treatment.

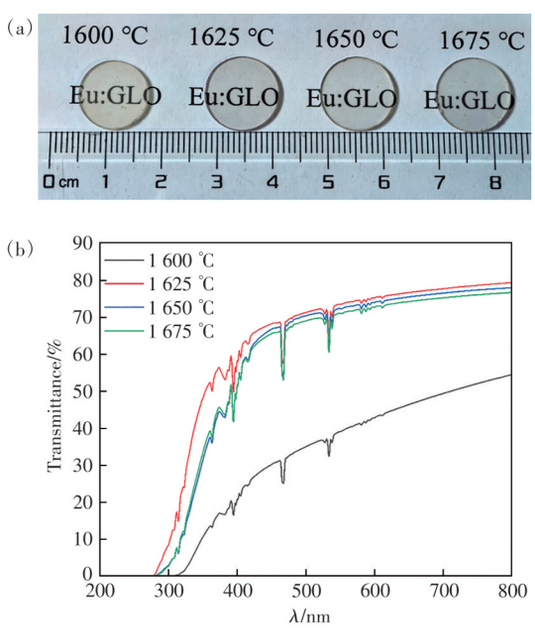

Fig. 6 Photograph(a) and in-line transmittance spectra(b) of the $Eu_{0.1}Gd_{0.6}Lu_{1.3}O_3$ ceramics pre-sintered at different temperatures for 2 h and HIP post-treated at 1 750 ℃ for 3 h under 176 MPa

Fig. 7 shows the excitation and emission spectra of the $Eu_{0.1}Gd_{0.6}Lu_{1.3}O_3$ ceramics. The excitation bands correspond to the energy transfer of Eu^{3+} ions. Among them, the peak at 323 nm corresponds to $^7F_0 \rightarrow {}^5L_8$ transition of Eu^{3+}, the peak at 394 nm corresponds to $^7F_0 \rightarrow {}^5L_6$ transition of Eu^{3+}, and the peak

at 468 nm corresponds to the $^5D_0 \rightarrow {}^7F_2$ transition of Eu^{3+}. The strongest luminescence peak of the ceramics locates at 611 nm, which corresponds to the $^5D_0 \rightarrow {}^7F_2$ transition. The intensity of most excitation peaks and all emission peaks of the ceramic in accordance with the ceramics' transmittance. The intensity of the excitation and luminescence spectra reaches its maximum at the pre-sintered temperature of 1 625 ℃, which is attributed to the highest in-line transmittance of the ceramics. The scattering from nanoscale residual pores becomes the main optical losses in ceramic luminescence.

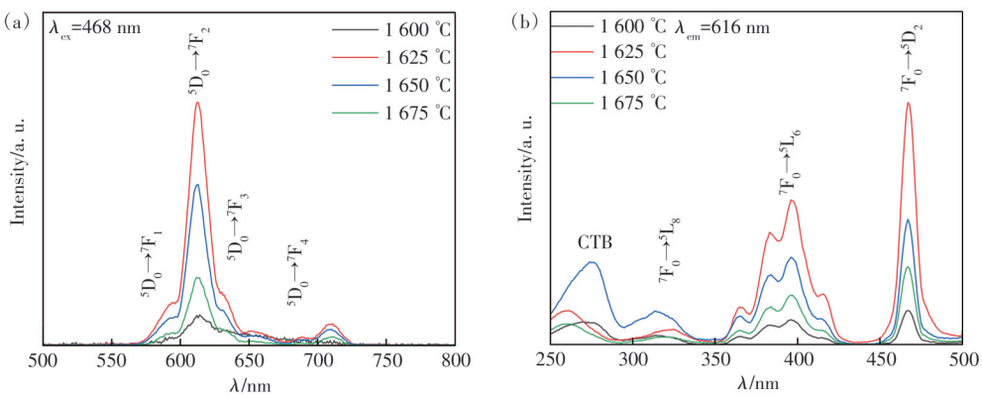

Fig. 7　PL(a) and PLE(b) spectra of the $Eu_{0.1}Gd_{0.6}Lu_{1.3}O_3$ ceramics pre-sintered at different temperatures for 2 h and HIP post-treated at 1 750 ℃ for 3 h under 176 MPa

Fig. 8 shows the XEL spectra of the $Eu_{0.1}Gd_{0.6}Lu_{1.3}O_3$ ceramics. The XEL spectrum of bismuth germinate ($Bi_4Ge_3O_{12}$, BGO) single crystal multiplies by 10 times is shown for comparison. The XEL luminescence spectra of the $Eu_{0.1}Gd_{0.6}Lu_{1.3}O_3$ ceramics consist of Eu^{3+} characteristic emission peaks. The main emission peak locates at 611 nm. It is the strong red light emitted by $^5D_0 \rightarrow {}^7F_2$ energy levels transition. The XEL spectra of the ceramics showed a trend of first increasing and then decreasing with the increase of sintering temperature. Above phenomena are arisen by the more optical losses, which lead to a decrease in the luminescence intensity of the ceramics. The highest intensity is found in the ceramics pre-sintered at 1 625 ℃ combined with HIP post-treatment. The light yield of the XEL emission of the $(Gd,Lu)_2O_3$:Eu is much higher than that of BGO, which makes the ceramics a promising material for X-ray imaging.

It is well known that Eu^{3+} ions are easy to capture an electron and reduce to Eu^{2+} due to its low oxidation potential[26]. Therefore, it is obvious to assume that Eu^{3+} itself is an effective electron trap in $(Gd,Lu)_2O_3$:Eu ceramics similar to Eu^{3+} doped in $(Y,Gd)_2O_3$[27]. The TSL glow curve of the $(Gd,Lu)_2O_3$:Eu ceramics (pre-sintered at 1 625 ℃ and HIP-ed at

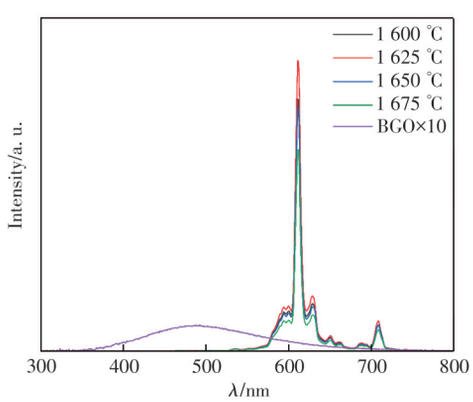

Fig. 8　XEL spectra of the $Eu_{0.1}Gd_{0.6}Lu_{1.3}O_3$ ceramics pre-sintered at different temperatures for 2 h and HIP post-treated at 1 750 ℃ for 3 h under 176 MPa of Ar and BGO×10

1 750 ℃) between 100 K and 400 K is given in Fig. 9. The glow curve of the sample presents one high peak at 178 K and two peaks of lower intensity at 253 K and 320 K, which is similar to that of $(Y,Gd)_2O_3$:Eu above 150 K[27]. Normally we consider the luminescence of the samples at 320 K may be related with the oxygen vacancies. Whereas the luminescence at 178 K is related to the defects arising from the change in the valence state of the Eu^{3+} ion itself. As can be seen from the Fig. 9, there are fewer oxygen vacancies present in $Eu_{0.1}Gd_{0.6}Lu_{1.3}O_3$ under the pre-sintering at 1 625 ℃ combined with HIP post-treatment. According to the Fig. 9 (b), the

radioluminescence intensity of the $Eu_{0.1}Gd_{0.6}Lu_{1.3}O_3$ ceramics increases continuously with the increase of temperature. The steep increase in intensity is observed in the range of 150 K to 250 K. This is consistent with the defects caused by the Eu ion in the TSL spectra corresponding to 178 K.

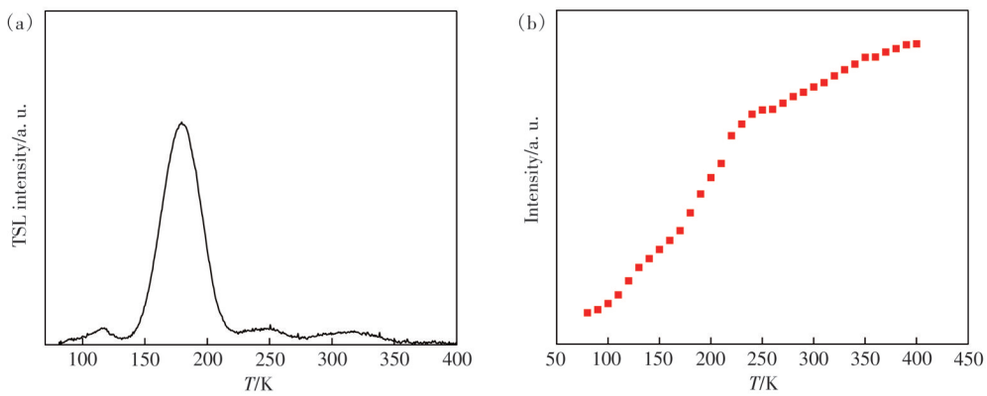

Fig. 9 Thermally stimulated luminescence curve(a) and radioluminescence curve(b) of the $Eu_{0.1}Gd_{0.6}Lu_{1.3}O_3$ ceramics pre-sintered at 1 625 ℃ for 2 h and HIP post-treated at 1 750 ℃ for 3 h under 176 MPa

4 Conclusion

In this paper, the pure cubic phase $Eu_{0.1}Gd_{0.6}Lu_{1.3}O_3$ powders were synthesized by co-precipitation method. The $Eu_{0.1}Gd_{0.6}Lu_{1.3}O_3$ ceramics with high in-line transmittance were prepared by vacuum pre-sintered at different temperatures combined with hot isostatic pressing (1 750 ℃ for 3 h, 176 MPa, Ar). The in-line transmittance of the $Eu_{0.1}Gd_{0.6}Lu_{1.3}O_3$ ceramics with the thickness of 1.2 mm is the highest at 1 625 ℃ for 2 h combined with HIP post-treatment, reaching a maximum of 75.2% at 611 nm. Moreover, the PLE/PL and XEL intensity of the ceramics shows the trend of first rising and then falling, which is consistent with the in-line transmittance. The ceramics show the strong red emission under X-ray excitation (the main peak is at 611 nm), which shows the potential of coupling with the silicon photodiode. Thus, the $Eu_{0.1}Gd_{0.6}Lu_{1.3}O_3$ ceramics have a good application prospect in X-ray imaging.

Response Letter is available for this paper at: http://cjl.lightpublishing.cn/thesisDetails#10.37188/CJL.20240186

References:

[1] ZHU D Y, NIKL M, CHEWPRADITKUL W, *et al*. Development and prospects of garnet ceramic scintillators: a review [J]. *J. Adv. Ceram.*, 2022, 11(12): 1825-1848.

[2] ZHU D Y, CHEN X P, BEITLEROVA A, *et al*. Influence of calcium doping concentration on the performance of Ce, Ca:LuAG scintillation ceramics [J]. *J. Eur. Ceram. Soc.*, 2022, 42(13): 6075-6084.

[3] TONG Y F, LI Y Y, SONG Q S, *et al*. Effects of Zr^{4+} and Hf^{4+} co-doping on luminescence and scintillation properties of LuYAG:Pr^{3+} single crystals grown by micro-pulling-down technique [J]. *J. Rare Earths*, 2024, 42(15): 654-658.

[4] RETIVOV V, DUBOV V, KUZNETSOVA D, *et al*. Gd^{3+} content optimization for mastering high light yield and fast $Gd_xAl_2Ga_3O_{12}$:Ce^{3+} scintillation ceramics [J]. *J. Rare Earths*, 2023, 41(12): 1911-1918.

[5] ZHU D Y, WU L X, BEITLEROVA A, *et al*. Compositional regulation of multi-component GYGAG:Ce scintillation ceramics: self-sintering-aid effect and afterglow suppression [J]. *J. Adv. Ceram.*, 2023, 12(10): 1919-1929.

[6] LEMPICKI A, BRECHER C, SZUPRYCZYNSKI P, *et al*. A new lutetia-based ceramic scintillator for X-ray imaging [J]. *Nucl. Instrum. Methods Phys. Res. Sect.* A: *Accel. Spectrom. Detect. Assoc. Equip.*, 2002, 488(3): 579-590.

[7] SHI Y, CHEN Q W, SHI J L. Processing and scintillation properties of Eu^{3+} doped Lu_2O_3 transparent ceramics [J]. *Opt. Mater.*, 2009, 31(5): 729-733.

[8] CAPPER P, RUDOLPH P. *Crystal Growth Technology*: *Semiconductors and Dielectrics* [M]. Weinheim: Wiley-VCH, 2010.

[9] KOPYLOV Y L, KRAVCHENKO V B, DULINA N A, *et al.* Fabrication and characterization of Eu^{3+}-doped Lu_2O_3 scintillation ceramics [J]. *Opt. Mater.*, 2013, 35(4): 812-816.

[10] QIN L S, WU Y T, SHI H S, *et al.* Effects of doping Lu_2O_3 into Gd_2O_3 on phase transformation and luminescence [J]. *IEEE Trans. Nucl. Sci.*, 2009, 56(5): 2979-2982.

[11] SEELEY Z M, DAI Z R, KUNTZ J D, *et al.* Phase stabilization in transparent Lu_2O_3: Eu ceramics by lattice expansion [J]. *Opt. Mater.*, 2012, 35(1): 74-78.

[12] SEELEY Z M, KUNTZ J D, CHEREPY N J, *et al.* Transparent Lu_2O_3: Eu ceramics by sinter and HIP optimization [J]. *Opt. Mater.*, 2011, 33(11): 1721-1726.

[13] SEELEY Z M, CHEREPY N J, PAYNE S A. Homogeneity of Gd-based garnet transparent ceramic scintillators for gamma spectroscopy [J]. *J. Cryst. Growth*, 2013, 379: 79-83.

[14] RÉTOT H, BLAHUTA S, BESSIÈRE A, *et al.* Improved scintillation time response in $(Lu_{0.5}Gd_{0.5})_2O_3$: Eu^{3+} compared with Lu_2O_3: Eu^{3+} transparent ceramics [J]. *J. Phy.* D: *Appl. Phys.*, 2011, 44(23): 235101.

[15] CAO M Q, XU J Y, HU C, *et al.* Fabrication and characterizations of $(Lu, Gd)_2O_3$: Eu scintillation ceramics [J]. *Ceram. Int.*, 2017, 43(2): 2165-2169.

[16] CAO M Q, HU Z W, MIVANOV*et al.* Effect of Gd substitution on structure and spectroscopic properties of $(Lu, Gd)_2O_3$: Eu ceramic scintillator [J]. *Opt. Mater.*, 2018, 76: 323-328.

[17] JING Y Q, LIU Q, SU S, *et al.* Fabrication of highly transparent Co: $MgAl_2O_4$ ceramic saturable absorber for passive *Q*-switching in 1.5 μm [J]. *J. Inorg. Mater.*, 2021, 36(8): 877-882.

[18] DU A C, DU Q Y, LIU X, *et al.* Ce:YAG transparent ceramics enabling high luminous efficacy for high-power LEDs/LDs [J]. *J. Inorg. Mater.*, 2021, 36(8): 883-892.

[19] SAKAR N, GERGEROGLU H, AKALIN S A, *et al.* Synthesis, structural and optical characterization of Nd:YAG powders *via* flame spray pyrolysis [J]. *Opt. Mater.*, 2020, 103: 109819.

[20] PING G X, WANG X Y, WU Y T, *et al.* Synthesis and luminescent characteristic of Eu^{3+}-doped $(Gd, Lu)_2O_3$ nanopowders [J]. *Opt. Mater.*, 2012, 34(4): 748-752.

[21] LIU Z Y, TOCI G, PIRRI A, *et al.* Fabrication, microstructures, and optical properties of Yb: Lu_2O_3 laser ceramics from co-precipitated nano-powders [J]. *J. Adv. Ceram.*, 2020, 9(6): 674-682.

[22] WANG Y B, HUANG X Y, CHENG Z Q, *et al.* Al_2O_3-Ce: YAG composite phosphor ceramics for white laser lighting: novel preparation and regulatable properties [J]. *J. Am. Ceram. Soc.*, 2023, 106(10): 5933-5943.

[23] HU D J, LI X Y, SNETKOV I, *et al.* Fabrication, microstructure and optical characterizations of holmium oxide (Ho_2O_3) transparent ceramics [J]. *J. Eur. Ceram. Soc.*, 2021, 41(1): 759-767.

[24] LI T S, LIU Q, ZHU D Y, *et al.* Fabrication and characterizations of Eu^{2+}-Dy^{3+} co-doped $SrAl_2O_4$ ceramics with persistent luminescence [J]. *J. Am. Ceram. Soc.*, 2023, 106(10): 5877-5886.

[25] ZHANG L X, LI X Y, HU D J, *et al.* Magneto-optical, thermal, and mechanical properties of polycrystalline $Tb_3Al_5O_{12}$ transparent ceramics [J]. *J. Am. Ceram. Soc.*, 2023, 106(9): 5311-5321.

[26] EYRING L, GSCHNEIDNER K A, LANDER G H. *Handbook on the Physics and Chemistry of Rare Earths* [M]. North-Holland, 1979.

[27] KÖSTLER W, WINNACKER A, ROSSNER W, *et al.* Effect of Pr-codoping on the X-ray induced afterglow of (Y, Gd)$_2O_3$:Eu [J]. *J. Phys. Chem. Solids*, 1995, 56(7): 907-913.

刘强(1964-),男,江苏镇江人,博士,教授,硕士生导师,2005 年于江苏大学获得博士学位,主要从事金属材料强韧化、透明陶瓷和发光材料的研究。
E-mail: lq88611338@163.com

李江(1977-),男,浙江绍兴人,博士,研究员,博士生导师,2007 年于中国科学院上海硅酸盐研究所获得博士学位,主要从事光学与光功能透明陶瓷方面的研究。
E-mail: lijiang@mail.sic.ac.cn